Role of Lewis acid sites of ZSM-5 zeolite on gaseous ozone abatement

Nicolas Brodu [a,b], Marie-Hélène Manero [a,b,*], Caroline Andriantsiferana [a,b], Jean-Stéphane Pic [c], Héctor Valdés [d]

[a] Université de Toulouse, INPT, UPS, Laboratoire de Génie Chimique, 4, Allée Emile Monso, F-31030 Toulouse, France
[b] CNRS, Laboratoire de Génie Chimique, F-31030 Toulouse, France
[c] Université de Toulouse, LISBP, UMR INSA/CNRS 5504 & UMR INSA/INRA 792, 135 Avenue de Rangueil, 31077 Toulouse Cedex 4, France
[d] Laboratorio de Tecnologías Limpias (F. Ingeniería), Universidad Católica de la Santísima Concepción, Alonso de Ribera 2850, Concepción, Chile

HIGHLIGHTS

We report the role played by acidic surface sites of ZSM-5 on ozone removal.
Ozone removal is mainly due to ozone decomposition on mild/strong Lewis acid sites.
Adsorbed oxygen species appear on ZSM-5 surface because of ozone decomposition.

Keywords:
Acidic sites
Chemical surface properties
Lewis acid sites
Ozone
Synthetic zeolites
ZSM-5 zeolite

ABSTRACT

In this work, chemical interactions between ozone and zeolite surface active sites are studied in order to propose a process for gaseous ozone removal. Synthetic ZSM-5 zeolites with three different Si/Al_2 ratios and similar specific surface areas and microporous volumes were used in this study. Zeolite samples were characterised using Fourier Transform InfraRed spectroscopy (FTIR) and pyridine sorption IR studies in order to determine acidic site concentrations and strength. Ozone removal experiments were conducted in a quartz fixed-bed flow reactor, at 20 °C and 101 kPa. Experiments using Diffuse Reflectance Infrared Fourier Transform Spectroscopy (DRIFTS) were conducted in order to identify adsorbed ozone and/or adsorbed oxygen species on zeolite surface. Pyridine IR measurements evidence two kinds of Lewis acid sites induced by extra-framework aluminium species and electronic aluminium defaults inside zeolite structure. Results obtained here evidence the important role of acidic surface sites of ZSM-5 zeolite on gaseous ozone removal. The total amount of removed ozone is found to be directly proportional to the total content of Lewis acid sites. DRIFTS experiments exhibit two bands around 800 and 1400 cm^{-1} that could correspond to adsorbed oxygen species linked to zeolite surface. DRIFTS experiments also exhibit a band around 1100 cm^{-1} that correspond to adsorbed ozone on the zeolite surface. Gaseous ozone removal using ZSM-5 zeolite could be largely attributed to ozone decomposition on Lewis acid sites and also to ozone adsorption on the surface of the zeolites.

1. Introduction

Tropospheric ozone is recognised to be harmful to human health, living organisms and the environment [1]. Long-term exposure to ozone can cause lung damage [2]. As well as being responsible of the urban smog in large cities, ozone is a pollutant involved in indoor air contamination. In working environments, the use of photocopiers, laser printers, fax machines cause ozone formation [3]. In water industry, ozone is applied for water disinfection and also for the oxidation of organic matter. Exhaust gases from such processes contain residual ozone, which could be above the acceptable value. The concern for maintaining air quality standards has led to the development of purification processes based on heterogeneous catalytic decomposition using microporous materials.

Activated carbons have been widely used for gaseous ozone elimination. However, long-term use of activated carbon leads to irreversible degradation of its physical and chemical surface properties [4]. Moreover, safety conditions have to be taken into consideration since activated carbon could be flammable. Synthetic zeolites appear as alternative materials for gaseous ozone removal from contaminated streams, due to their high thermal and chemical stability. They have been applied as catalysts in advanced oxidation processes in combination with ozone for the oxidation of volatile organic compounds from industrial emissions [5–7]. Concerning to gaseous ozone abatement over zeolites at ambient

Corresponding author at: Université de Toulouse, INPT, UPS, Laboratoire de Génie Chimique, 4, Allée Emile Monso, F-31030 Toulouse, France. Tel.: +33 5 34323684; fax: +33 5 34323697.
E-mail address: marie-helene.manero@iut-tlse3.fr (M.-H. Manero).

conditions, there are only few reported investigations [8–11]. Two mechanisms are proposed: decomposition on strong Lewis acid sites and adsorption of ozone on weak acidic sites. Nevertheless, there are still some doubts about the nature of chemical interactions between ozone and zeolite surface active sites.

In order to understand the involved mechanisms of gaseous ozone removal on synthetic zeolites, the influence of chemical surface properties of synthetic zeolites is studied here. Infrared studies are used to evidence the main contributions of hydroxyl stretching bands of ZSM-5 zeolite. Moreover, Fourier Transform InfraRed spectroscopy (FTIR) analysis of pyridine adsorption elucidate the nature and strength of zeolite acidic sites; and Diffuse Reflectance Infrared Fourier Transform Spectroscopy (DRIFTS) allows to identify the nature of the surface chemical groups, indicating ozone adsorption and/or decomposition on zeolite surface sites.

2. Material and methods

2.1. Materials

ZSM-5 zeolites with three different Si/Al_2 ratios were provided in pellet forms by Tosoh and Zeochem. ZSM-5 zeolite exhibits a three-dimensional pore network with 10-membered straight and sinusoidal ring channels and apertures of 5.3×5.6 Å and 5.1×5.5 Å, respectively [12]. Zeolite samples used in this study were ground and sieved to 0.300–0.425 mm; then were rinsed with ultra pure water, oven-dried at 125 °C for 24 h, and stored in desiccators until their further use. Samples are named according to the Si/Al_2 ratio 78, 360, and 2100 as Z-78, Z-360 and Z-2100, respectively.

Ozone was generated from instrumental dry air supplied by PRAXAIR, using an AZCOZON A-4 ozone generator (AZCO Industries, Vancouver, BC, Canada) rate at 4 g O_3 h^{-1}. Ultrapure water ($\geqslant$18.0 MΩ cm) was obtained from an EASY pure® RF II system (Barnstead Thermolyne Corp., Dubuque, USA).

2.2. Experimental set up

Ozone removal experiments were conducted in a quartz U-shaped fixed-bed flow reactor (4 mm ID), at 20 °C (±1 °C) and 101 kPa [13]. The reactor was charged with 0.100 g of zeolite sample. A thermal out-gassing procedure was applied prior to the experiments, using an Argon flow (100 cm^3 min^{-1}) during 2 h at 500 °C (heating rate 10 °C min^{-1}). Ozone outlet concentration was recorded continuously using a BMT 964 BT ozone analyser (BMT Messtechnik GmbH, Berlin, Germany). The exhaust gas stream was sent to an ozone trap before discharging to ambient air. The flow rate was measured at 20 °C and 101 kPa and fixed at 50 cm^3 min^{-1}. Ozone inlet concentration was ranged from 6 to 26 g m^{-3}. Total removed ozone, Q (mgO_3 g^{-1}), was calculated from a mass balance between the inlet and outlet reactor streams using the following equation:

$$Q = \frac{FC_{O_{3in}}}{m} \int_0^{t_s} \left(1 - \frac{C_{O_{3t}}}{C_{O_{3in}}}\right) dt \quad (1)$$

where m is the zeolite mass (g); $C_{O_{3in}}$ is the inlet concentration of ozone (g m^{-3}); F is the volumetric flow rate (m^3 min^{-1}) and t_s is the time needed to reach the zeolite saturation with ozone; $C_{O_{3t}}$ is the ozone concentration as a function of time (g m^{-3}).

2.3. Characterisation of zeolite samples

Specific surface areas and pore volumes were obtained by nitrogen adsorption–desorption at −196 °C using a Micromeritics ASAP 2010 instrument. Prior to nitrogen adsorption, zeolite samples were outgassed at 90 °C for 1 h and then 4 h at 350 °C. Specific surface areas (S_{BET}) were calculated from nitrogen adsorption isotherms, using the Brunauer–Emmett–Teller (BET) equation. Micropore (V_{micro}) and mesopore (V_{meso}) volumes were determined by applying the Horvath–Kawazoe (HK) and Barrett, Joyner, and Halenda (BJH) methods, respectively [14,15]. Table 1 summarises the physicochemical characteristics of the zeolite samples. As it can be seen the three ZSM-5 zeolite samples selected in this study have similar physical properties.

Hydroxyl surface groups of ZSM-5 were characterised by infrared spectroscopy (IR), using a NICOLET MAGNA IR 550 spectrometer. Zeolite samples were pressed into thin wafers (10 mg cm^{-2}) and were activated in situ in the IR cell by applying air flow (1 cm^3 s^{-1}) at 500 °C for 12 h and then under vacuum (1.33×10^{-4} Pa) at 400 °C for 1 h. Spectra were recorded at 20 °C with a resolution of 2 cm^{-1} in the region ranging from 3500 to 3800 cm^{-1}.

Standard assays using temperature-programmed desorption of carbon dioxide (CO_2-TPD) were applied in order to determine the total number and strength of basic sites as described elsewhere [9]. No peaks were observed after the CO_2-TPD assays. These results suggest that ZSM-5 zeolites have not basic sites.

Acidic properties of three ZSM-5 zeolite samples were investigated by FTIR spectroscopy using pyridine as a probe molecule (99.5% purity supplied by Fluka). Measurements were performed on a NICOLET MAGNA IR 550 spectrometer equipped with a vacuum cell. Zeolite samples were pressed into thin wafers (10 mg cm^{-2}) and were activated in situ in the IR cell, passing air flow (1 cm^3 s^{-1}) at 450 °C for 12 h and then applying vacuum (1.33×10^{-4} Pa) at 400 °C for 1 h. Pyridine was adsorbed at 150 °C. A progressive thermal desorption procedure (steps from 150 to 450 °C) was conducted in order to determine the acidity strength of Lewis and Brønsted acid sites by evaluating the amount of remaining adsorbed pyridine as temperature increases. Lewis and Brønsted acid sites detected above 350 °C are considered as strong acidic sites. Spectra were recorded with a resolution of 2 cm^{-1} in the region ranging from 1400 to 1650 cm^{-1}. Brønsted (PyH) and Lewis (PyL) acid site concentrations were calculated by the integration of the IR bands at 1545 cm^{-1} (1.13 cm mol^{-1} as a molar absorption coefficient) and at 1450 cm^{-1} (1.28 cm mol^{-1} as a molar absorption coefficient), respectively [16].

2.4. DRIFTS experiments

Diffuse Reflectance Infrared Fourier Transform Spectroscopy (DRIFTS) experiments were conducted in order to identify adsorbed ozone and/or adsorbed active oxygen species on the zeolite surface. DRIFTS measurements were carried out using a Nicolet 6700 FTIR spectrometer equipped with a smart collector diffuse reflectance mirror system and a high-temperature/high-pressure DRIFTS cell (Thermo Scientific) as described in a former publication [9].

3. Results and discussion

3.1. Chemical surface characterisation of zeolite samples

3.1.1. IR identification of hydroxyl groups

Fig. 1 displays IR spectra of the zeolite samples in the range from 3500 to 3800 cm^{-1}. Four hydroxyl bands appear in ZSM-5

Table 1
Physical–chemical properties of ZSM-5 samples.

Zeolites	S_{BET} (m^2 g^{-1})	V_{micro} (cm^3 g^{-1})	V_{meso} (cm^3 g^{-1})	Si/Al_2 ratio
Z-78	361	0.14	0.13	78
Z-360	309	0.12	0.11	360
Z-2100	308	0.11	0.07	2100

spectra. The bands at 3740 and 3720 cm^{-1} correspond to silanol groups (SiOH). The first band was previously attributed to amorphous silica, whereas the second is ascribed to terminal silanol groups in the zeolite structure as it was observed on BEA zeolites [17]. The IR signal around 3660–3690 cm^{-1} could be assigned to extra-framework aluminium species (EFAL) or partially hydrolysed aluminium species, bound to the zeolite framework via one or two oxygen bonds [18]. The area of IR band between 3660 and 3690 cm^{-1} increases as follows: Z-2100 (0.26 a.u.) < Z-360 (0.42 a.u.) < Z-78 (2.10 a.u.), suggesting that Z-78 sample contains more EFAL species than the two other zeolites as it was expected. In the Z-78 IR spectrum the band that appears at 3610 cm^{-1} could correspond to bridging hydroxyl groups Si(OH)Al which has been considered as the strongest Brønsted acid sites [16].

3.1.2. Characterisation of zeolite surface acidity

Fig. 2 shows IR spectra after pyridine desorption at different temperatures. Concerning to Lewis acid sites, a band at 1444 cm^{-1} is observed in all the ZSM-5 zeolites. Another band at 1454 cm^{-1} is only visible on Z-78. The presence of these bands can be attributed to two types of Lewis acid sites. Lewis acid sites could be due not only to the presence of EFAL but also could be related to electronic defaults in the framework aluminium (FAL) [17]. Moreover, IR experiments on the desorption of pyridine from Z-78 evidence that the band at 1444 cm^{-1} is removed when the temperature is increased from 150 to 350 °C. However, the band at 1454 cm^{-1} is eliminated when the temperature is risen up to 350 °C. These results indicate that the band at 1454 cm^{-1} could correspond to Lewis acid sites related to FAL and the band at 1444 cm^{-1} could be associated to EFAL. These assignments are in agreement with those proposed by Marques et al. [17] who identified EFAL as a weaker Lewis acid site than FAL.

Table 2 summarises the concentration of Lewis and Brønsted acid sites, determined after the integration of the area under the bands at 1444 and 1454 cm^{-1} for the Lewis acid sites and at 1546 cm^{-1} for the Brønsted acid sites (see Fig. 2). Results reveal that Z-78 is the most acidic ZSM-5 studied here followed by Z-360 sample and then by Z-2100 sample. As it can be expected, the content of Brønsted and Lewis acid sites decreases when the Si/Al_2 ratio increases. Moreover, mild Lewis acid sites, indicated in Table 2, could be related to EFAL, whereas the strongest Lewis acid sites could be related to FAL. Hence, EFAL species represent most of the total Lewis acid sites of the whole zeolite samples.

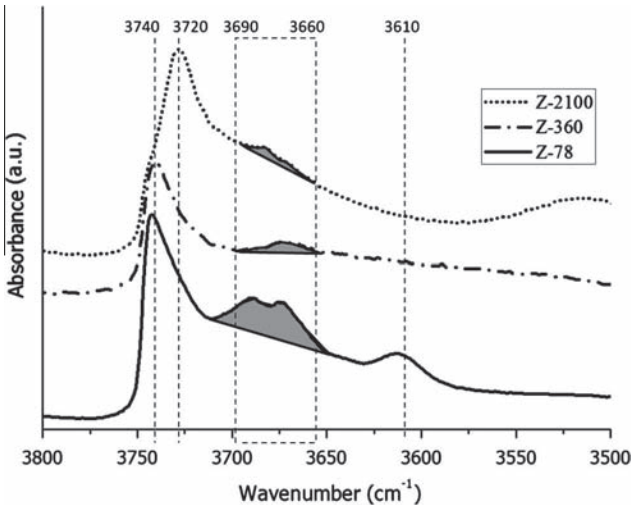

Fig. 1. IR spectra of hydroxyl region of ZSM-5 zeolites: Z-78, Z-360, Z-2100. Activation conditions: 12 h in air flow (1 $cm^3 s^{-1}$) at 500 °C and then using vacuum (1.33×10^{-4} Pa) at 400 °C for 1 h. NB: The curves are offset for a better readability.

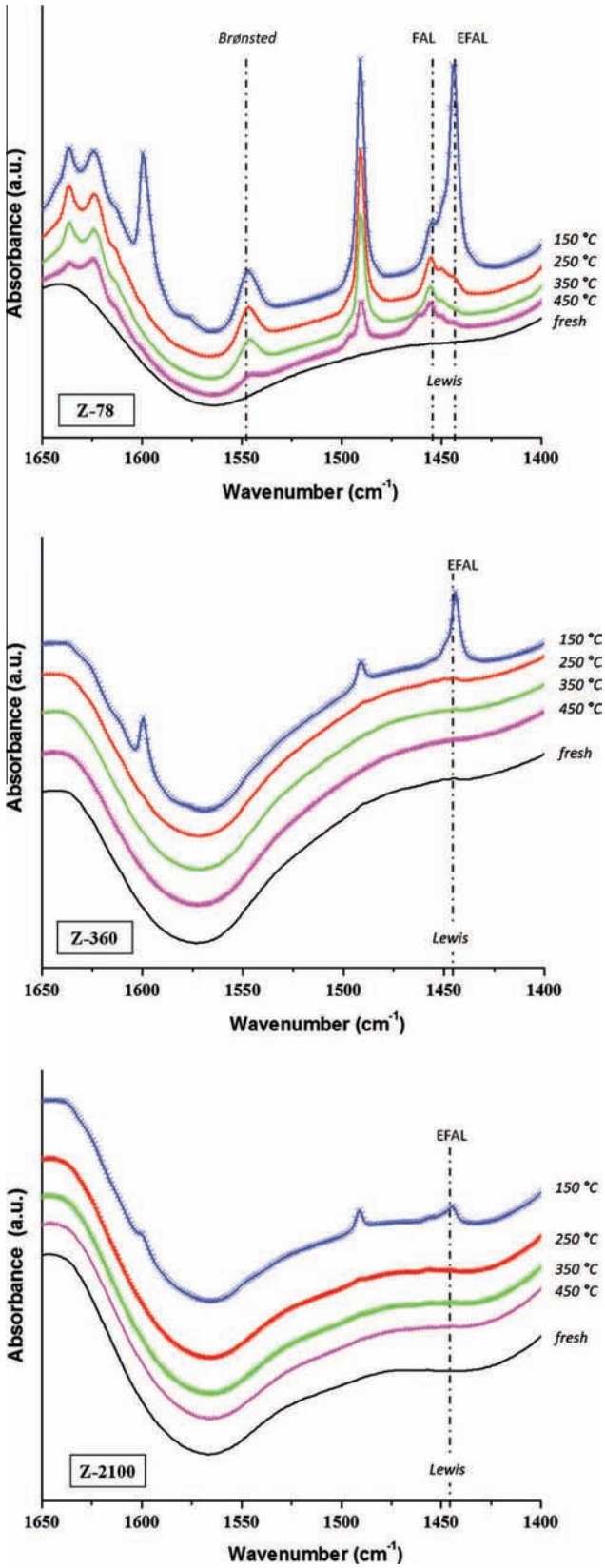

Fig. 2. Acidity characterisation by IR spectroscopy of ZSM-5 zeolites: Z-78, Z-360, Z-2100. IR spectra after pyridine adsorption and desorption at different temperatures. NB: the curves are offset for a better readability.

Table 2
Concentration and strength of Brønsted and Lewis acid sites obtained from IR spectra after adsorption/desorption of pyridine. Mild acid sites are the remained acid sites after a thermal desorption between 150 and 350 °C. Strong acid sites are those remained after a thermal desorption above 350 °C.

Zeolites	Lewis acid sites			Brønsted acid sites		
	Content	Strength		Content	Strength	
	(μmol g^{-1})	Strong (%)	Mild (%)	(μmol g^{-1})	Strong (%)	Mild (%)
Z-78	231	17	83	96	57	43
Z-360	53	0	100	5	0	100
Z-2100	28	11	89	4	0	100

3.2. Interactions of ozone on zeolite in the fixed-bed reactor

Fig. 3 shows the evolution of the outlet ozone dimensionless concentration as a function of time for an inlet ozone concentration of 6.5 g m^{-3}. $C_{o_{3t}}$ and $C_{o_{3in}}$ are the concentration of ozone as a function of time in the outlet and inlet reactor streams, respectively. Experimental results indicate that higher ozone elimination is obtained using Z-78 compared to Z-360 and Z-2100 samples. The highest ozone removal is observed over the most acidic ZSM-5 zeolite (Z-78). The least acidic zeolite sample (Z-2100), with the highest Si/Al_2 ratio, shows the lowest ozone elimination. These results indicate the important role played by acidic surface sites of ZSM-5 zeolites on ozone removal. In all cases the rate of ozone removal on ZSM-5 samples is very high in the first few minutes. This is then followed by a slower rate that gradually reaches the inlet concentration of ozone, leading probably to the deactivation of zeolites. The first fast removal stage could be related to the initial adsorption of ozone molecules on the active sites on ZSM-5 surface, followed by slow ozone transformation on acidic surface sites.

The plot shown in Fig. 4 evidences the effect of zeolite Lewis acid concentrations on ozone removal. Linear relations between the total ozone consumption (calculated using Eq. (1)) and the total concentration of Lewis acid sites are obtained for each value of the assessed inlet concentration of ozone. Results indicate that the increase in ozone inlet concentration increase the amount of removed ozone per Lewis acid site content. Due to its resonance structure ozone could act as a Lewis base, interacting with Lewis acid surface sites [19]. It has been previously reported that ozone could be decomposed to form atomic oxygen (O) on strong Lewis acid sites and could be adsorbed as a molecule on weak Lewis acid sites [10,20]. However, pyridine adsorption IR results obtained at 150 °C identified only mild and strong Lewis acid sites. Thus, in the presence of ZSM-5 zeolites, gaseous ozone would be mainly eliminated by a decomposition mechanism on strong Lewis acid sites. Otherwise, no relation is found between Brønsted acid sites and the quantity of consumed ozone, as it was already reported in a former study on natural zeolites [10].

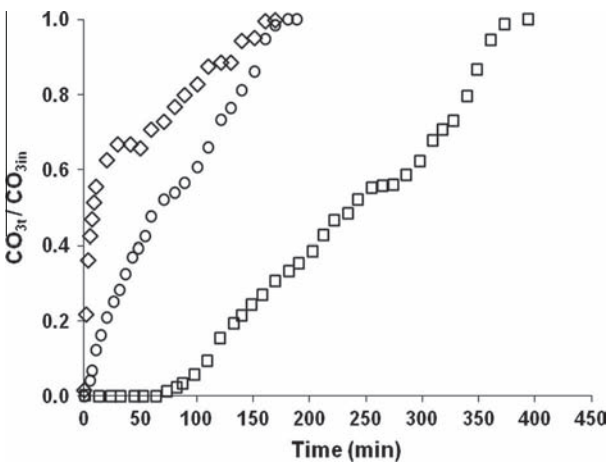

Fig. 3. Influence of chemical surface properties of ZSM-5 zeolites on ozone removal: (□) Z-78, (○) Z-360, (◇) Z-2100. Operating conditions: 0.1 g of zeolite; 6.5 g m^{-3} of inlet ozone concentration; 50 cm^3 min^{-1}; 101 kPa; 20 °C; $C_{o_{3t}}/C_{o_{3in}}$ represents dimensionless concentration of ozone.

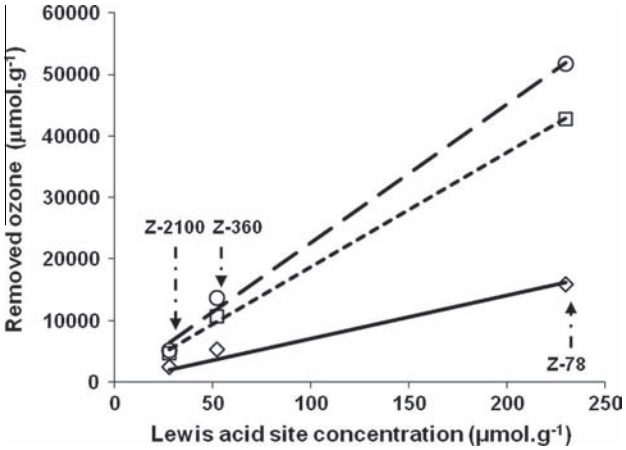

Fig. 4. Relation between the amount of removed ozone and Lewis acid concentration for three different inlet concentration of ozone: (◇) 6 g m^{-3}, (□) 15 g m^{-3}, (○) 24 g m^{-3}.

These results were previously observed on Chilean natural zeolites [10], alumina [21] and on ZSM-5 zeolite [11]. A similar mechanism used to describe ozone interaction with metal oxides [21,22] could help to explain ozone interaction with Lewis acid surface sites of ZSM-5 zeolites (Z–Al), as follows:

$$O_3 + Z{-}Al \rightarrow Z{-}Al\cdots O + O_2 \quad (2)$$

$$O_3 + Z{-}Al\cdots O \rightarrow Z{-}Al\cdots O_2 + O_2 \quad (3)$$

$$Z{-}Al\cdots O_2 \rightarrow Z{-}Al + O_2 \quad (4)$$

Lewis acid sites could convert ozone into atomic oxygen species (Z–Al···O). After a series of reactions, Lewis acid sites could be regenerated and be available for a new catalytic cycle. However, it has been noticed that Eq. (3) is longer and more difficult to occur than the other steps [22]. A progressive deactivation of ZSM-5 could occur due to this step as observed in Fig. 3. This assumption was proposed in case of ozone interaction with alumina [23].

Fig. 5 presents DRIFTS spectra of Z-78, the most reactive ZSM-5 toward ozone. DRIFTS spectra were recorded in the absence of ozone (t = 0 min) and after different times of ozone exposure (3, 15, 26 and 32 min). The main bands are observed in following ranges: 780–820 cm^{-1}, 1040–1060 cm^{-1}, 1080 cm^{-1}, 1140 cm^{-1} and 1390 cm^{-1}. The intensities of four spectra bands were widely affected by ozone interaction with Z-78 zeolite surface. The first observed band falls in the range of adsorbed peroxide ($Z{-}Al\cdots O_2$) as it has been detected between 640–970 cm^{-1} on oxide surfaces by other researchers [24]. The band at 1040–1060 cm^{-1}, at

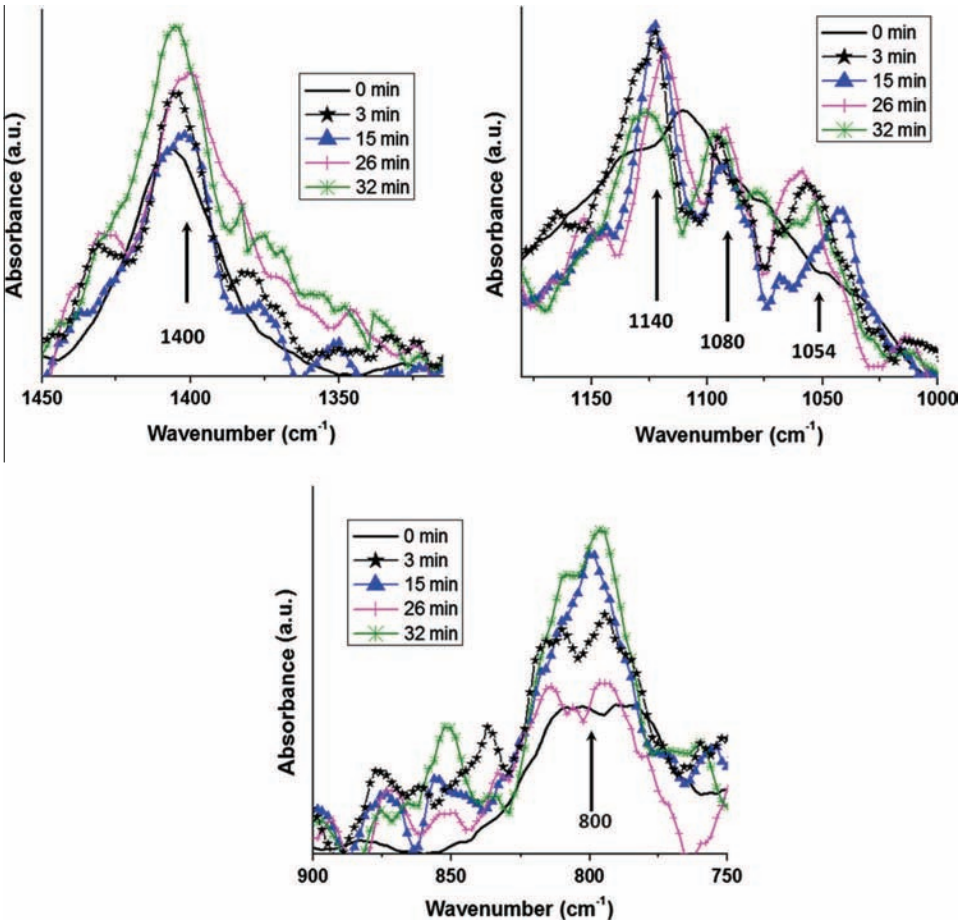

Fig. 5. DRIFT spectra of Z-78 zeolite sample during gaseous ozone removal. Operating conditions: 0.05 g of zeolite (1% w); 0.65 g m^{-3} of inlet ozone concentration; 100 cm^3 min^{-1}; 101 kPa; 20 °C.

1080 cm^{-1} and at 1140 cm^{-1} could be related to adsorbed molecular ozone on weak Lewis acid sites [25]. The band at 1400 cm^{-1} has been assigned to atomic oxygen attached to strong Lewis acid sites [21,26]. This surface site has been claimed as responsible of ozone decomposition on natural zeolite [9]. Moreover, the presence of the band frequency related to adsorbed peroxide would indicate that ozone decomposition takes place as described by Eqs. (2)–(4).

IR bands related to molecular adsorbed ozone do not show important differences with ozonation time; whereas the band area associated to the formation of atomic oxygen and peroxides species seem to fluctuate. When the outlet ozone concentration reaches the inlet ozone concentration (t = 32 min), these bands are still observed and their intensities are the highest. At the end of ozone exposure, the presence of both adsorbed species, peroxide (Z–Al···O_2) and atomic oxygen (Z–Al···O) could confirm that the strong Lewis acid sites are no longer available as ozone exposure time increases. This result would probably be consistent with the hypothesis of zeolite surface site deactivation.

4. Conclusions

IR investigation of pyridine adsorption/desorption allows to quantify mild and strong Lewis and Brønsted acid sites present on ZSM-5 zeolites. Extra-framework aluminium species (EFAL) and electronic defaults in the framework aluminium (FAL) are identified in this study as the main Lewis acid sites of ZSM-5 zeolites. Gaseous ozone elimination is directly related to the concentration of Lewis acid sites. DRIFT results using Z-78 zeolite sample confirm that gaseous ozone is eliminated by two mechanisms: mainly by decomposition on strong Lewis acid sites and by adsorption on weak Lewis acid sites. Moreover, DRIFT experiments reveal adsorbed peroxide and atomic oxygen species on zeolite surface. ZSM-5 zeolites and ozone could be coupled in a new kind of heterogeneous catalytic ozonation for volatile organic compounds (VOCs) removal from industrial emissions since ozone decomposition by-products such as atomic oxygen and peroxide species are formed on zeolite surface.

Acknowledgements

Authors gratefully acknowledge ANR (Grant No. ANR-10-ECOT-011-01), CONICYT, FONDECYT/Regular (Grant No. 1130560) and ECOS/CONICYT Program (Grant No. C11E08), for their financial support. N. Brodu wishes to thank Mr. V. Solar from *Laboratorio de Tecnologías Limpias, Universidad Católica de la Santísima Concepción* for his valuable collaboration, Mr. S. Alejandro from *Programa de Doctorado en Ingeniería Química, Universidad de Concepción* who conducted the DRIFT analysis and *Grupo de Catálisis y Carbones, Universidad de Concepción* for their valuable contributions.

References

[1] J.N. Cape, Surface ozone concentrations and ecosystem health: past trends and a guide to future projections, Sci. Total Environ. 400 (2008) 257–259.
[2] M.S. O'Neill, D. Loomis, V.H. Borja-Aburto, Ozone, area social conditions, and mortality in Mexico City, Environ. Res. 94 (2004) 234–242.

[3] S.T. Oyama, Chemical and catalytic properties of ozone, Catal. Rev.: Sci. Eng. 42 (2000) 279–322.
[4] H. Valdés, M. Sánchez-Polo, J. Rivera-Utrilla, C.A. Zaror, Effect of ozone treatment on surface properties of activated carbon, Langmuir 18 (2002) 2111–2116.
[5] C.W. Kwong, C.Y.H. Chao, K.S. Hui, M.P. Wan, Catalytic ozonation of toluene using zeolite and MCM-41 materials, Environ. Sci. Technol. 42 (2008) 8504–8509.
[6] P. Monneyron, M.H. Manero, J.S. Pic, A combined selective adsorption and ozonation process for VOCs removal from air, Can. J. Chem. Eng. 85 (2007) 326–332.
[7] N. Brodu, H. Zaitan, M.-H. Manero, J.-S. Pic, Removal of volatile organic compounds by heterogeneous ozonation on microporous synthetic alumino silicate, Water Sci. Technol. 66 (2012) 2020–2026.
[8] N. Kumar, P. Konova, A. Naydenov, T. Salmi, D.Y. Murzin, T. Heikilla, V.P. Lehto, Ag-modified H-Beta, H-MCM-41 and SiO_2: influence of support, acidity and Ag content in ozone decomposition at ambient temperature, Catal. Today 119 (2007) 342–346.
[9] H. Valdés, S. Alejandro, C.A. Zaror, Natural zeolite reactivity towards ozone: the role of compensating cations, J. Hazard. Mater. 227–228 (2012) 34–40.
[10] S. Alejandro, H. Valdés, C.A. Zaror, Natural zeolite reactivity towards ozone: the role of acid surface sites, J. Adv. Oxid. Technol. 14 (2011) 182–189.
[11] P. Monneyron, S. Mathe, M.H. Manero, J.N. Foussard, Regeneration of igh silica zeolites via advanced oxidation processes – A preliminary study about adsorbent reactivity toward ozone, Chem. Eng. Res. Des. 81 (2003) 1193–1198.
[12] D.W. Breck, Zeolite Molecular Sieves: Structure, Chemistry and Use, John Wiley & Sons, Inc., New York, 1974.
[13] S. Alejandro, H. Valdés, M.-H. Manero, C.A. Zaror, BTX abatement using Chilean natural zeolite: the role of Brønsted acid sites, Water Sci. Technol. 66 (2012) 1759–1765.
[14] G. Horvath, K. Kawazoe, Method for the calculation of effective pore size distribution in molecular sieve carbon, J. Chem. Eng. Jpn. 16 (1983) 470–475.
[15] E.P. Barrett, L.G. Joyner, P.P. Halenda, The determination of pore volume and area distributions in porous substances. I. Computations from nitrogen isotherms, J. Am. Chem. Soc. 73 (1951) 373–380.
[16] M. Guisnet, P. Ayrault, C. Coutanceau, M. Fernanda Alvarez, J. Datka, Acid properties of dealuminated beta zeolites studied by IR spectroscopy, J. Chem. Soc., Faraday Trans. 93 (1997) 1661–1665.
[17] J.P. Marques, I. Gener, P. Ayrault, J.C. Bordado, J.M. Lopes, F.R. Ribeiro, M. Guisnet, Dealumination of HBEA zeolite by steaming and acid leaching: distribution of the various aluminic species and identification of the hydroxyl groups, C. R. Chim. 8 (2005) 399–410.
[18] X.-Z. Jiang, In situ FTIR studies of extraframework aluminum bound methoxy species in H-ZSM-5 zeolites, J. Mol. Catal. A: Chem. 121 (1997) 63–68.
[19] B. Kasprzyk-Hordern, M. Ziolek, J. Nawrocki, Catalytic ozonation and methods of enhancing molecular ozone reactions in water treatment, Appl. Catal., B: Environ. 46 (2003) 639–669.
[20] C.W. Kwong, C.Y.H. Chao, K.S. Hui, M.P. Wan, Removal of VOCs from indoor environment by ozonation over different porous materials, Atmos. Environ. 42 (2008) 2300–2311.
[21] J.M. Roscoe, J.P.D. Abbatt, Diffuse reflectance FTIR study of the interaction of alumina surfaces with ozone and water vapor, J. Phys. Chem. A 109 (2005) 9028–9034.
[22] W. Li, S.T. Oyama, Mechanism of ozone decomposition on a manganese oxide catalyst. 2. Steady-state and transient kinetic studies, J. Am. Chem. Soc. 120 (1998) 9047–9052.
[23] R.C. Sullivan, T. Thornberry, J.P.D. Abbatt, Ozone decomposition kinetics on alumina: effects of ozone partial pressure, relative humidity and repeated oxidation cycles, Atmos. Chem. Phys. 4 (2004) 1301–1310.
[24] M. Che, A.J. Tench, Characterization and reactivity of molecular oxygen species on oxide surfaces, in: D.D. Eley, H. Pines, P.B. Weisz (Eds.), Advances in Catalysis, Academic Press, New York, 1983, pp. 1–148.
[25] K.M. Bulanin, J.C. Lavalley, A.A. Tsyganenko, IR spectra of adsorbed ozone, Colloids Surf., A 101 (1995) 153–158.
[26] C.Y.H. Chao, C.W. Kwong, K.S. Hui, Potential use of a combined ozone and zeolite system for gaseous toluene elimination, J. Hazard. Mater. 143 (2007) 118–127.